Pharm Res (2018) 35: 1
https://doi.org/10.1007/s11095-017-2311-3

RESEARCH PAPER

A Nanocarrier Skin-Targeted Drug Delivery System using an Ascorbic Acid Derivative

Yutaka Inoue [1] • Mitsue Hibino [1] • Isamu Murata [1] • Ikuo Kanamoto [1]

Received: 24 August 2017 / Accepted: 12 November 2017 / Published online: 28 December 2017

ABSTRACT

Purpose As trisodium L-ascorbyl 2-phosphate 6-palmitate (APPS), an ascorbic acid derivative, is an amphiphilic substance, it forms micelles in aqueous solutions. Micelles are used as drug carriers and can emulsify drugs that are poorly soluble in water, such as nadifloxacin (NDFX). The purpose of this study was to prepare nanocarriers using APPS to carry NDFX into Yucatan micropig skin.

Methods After synthesis of the NDFX nanoparticles by using the hydration method, physical evaluations were carried out that included assessments of particle size and zeta potential, encapsulation efficiency, particle structure by transmission electron microscopy, ^{31}P–NMR spectra, and particle stability. Functional evaluations of the nanoparticles included 2,2-diphenyl-1-picrylhydrazyl (DPPH) radical scavenging assays, skin penetration tests, and fluorescence microscopy observations.

Results The encapsulation efficiency of NDFX in the nanoparticles was approximately 75%. With added magnesium chloride, the nanoparticles remained stably dispersed in aqueous solution for at least 14 days at 25°C under protection from light. In addition, the nanoparticle formulation improved the skin permeability of NDFX.

Conclusion APPS-derived nanoparticles were shown to be useful as skin-targeting nanocarriers.

KEY WORDS ascorbic acid derivative · nadifloxacin · nanoparticle · nicelle · skin permeation

✉ Yutaka Inoue
yinoue@josai.ac.jp

[1] Laboratory of Drug Safety Management, Faculty of Pharmacy and Pharmaceutical Sciences, Josai University, 1-1 Keyakidai, Sakado-shi, Saitama 3500295, Japan

ABBREVIATIONS

APPS	Trisodium L-ascorbyl 2-phosphate 6-palmitate
DDSs	Drug delivery systems
DLS	Dynamic light scattering
DPPH	2,2-diphenyl-1-picrylhydrazyl
DSPE-PEG 2000	Distearoyl phosphatidylethanolamine-polyethylene glycol 2000
EE%	Encapsulation efficiency rate
HPLC	High-performance liquid chromatography
IC_{50}	50% inhibitory concentration
IPM	Isopropyl myristate
NDFX	Nadifloxacin
PEG	Polyethylene glycol
TEM	Transmission electron microscopy
YMP	Yucatan micropig

INTRODUCTION

Nanoparticles exhibit novel physical properties unlike those of conventional preparations; therefore, attention has been focused on the use of these particles as drug delivery systems (DDSs) (1,2). Components such as cosmetic ingredients, commonly used drugs, and novel nucleic acid-based pharmaceutical agents have been incorporated into nanoparticles or have been carried on their surface. Studies have indicated that this approach improves the absorbance and retention of active ingredients at target sites, reducing adverse reactions and improving stability in comparison to that of existing products. In addition, an increased drug load and penetration of cell membranes can result in increased bioavailability, and these characteristics can minimize individual differences and *in vivo* variations in pharmacokinetics (3,4). Moreover, nanoparticles are used to solubilize poorly water-soluble drugs. Lipophilic drugs can be emulsified using a surfactant (5). Emulsions exhibit various physical properties, depending on the type of

emulsion, particle size, and the composition of the oil and water phases. Thus, each emulsion can be used for different purposes (6–8). In addition, emulsions are used in cosmetics and pharmaceuticals, and an emulsion is a particularly useful way to prepare a formulation that targets the skin. Micelles and liposomes e.g. are studied for emulsions as skin-targeted nanocarriers. Nanocarrier is a drug transport system to a target site by adhering or adsorbed a drug on the surface or inside of the particle (3). Skin-targeted nanocarriers promote better drug delivery to a topical site compared to other DDS substrates such as suspensions and gels. And nanocarriers containing a lipophilic substance with affinity for the skin lipid improve to penetrate the drug into the skin barrier (9–12). However, emulsions are thermodynamically unstable; so the use of nanoparticles helps an emulsion retain its low viscosity and long-term stability. Over the past few years, the preparation of nanoemulsions has become easier, thanks to advances in high-pressure homogenizers and ultrasonic homogenizers with strong shearing forces (13). In addition, antioxidants have been added to nanoparticles to stably incorporate drugs into the nanoparticles and to protect them from oxidation. Sodium ascorbate and α-tocopherol were used in combination to prevent oxidation of a nanoemulsion containing astaxanthin, and this combination successfully inhibited the oxidation of astaxanthin (14).

Ascorbic acid is a water-soluble vitamin, which can, for example, inhibit melanin generation, promote collagen synthesis, and act as an antioxidant. Ascorbic acid is widely used as a pharmaceutical additive, cosmetics ingredient, and food additive. Nevertheless, it is susceptible to heat and light in aqueous solution and it readily oxidizes and decomposes. Various ascorbic acid derivatives have been synthesized to address these flaws and improve the stability of ascorbic acid (15,16). L-ascorbyl-6-stearate and L-ascorbyl-6-palmitate are fat-soluble ascorbic acid derivatives. These derivatives have long been used as antioxidative components in cosmetics creams and emulsions, and they have also been used as antioxidant food additives in edible fats and oils. Thus, these additional properties of ascorbic acid derivatives should facilitate their use in various fields (17,18). However, fat-soluble ascorbic acid derivatives are not used as principal components in quasi-drugs or as pharmaceutical additives, although some studies have examined such uses (19,20). Trisodium L-ascorbyl 2-phosphate 6-palmitate (APPS) is an ascorbyl phosphate derivative incorporating palmitic acid, resulting in a new, water-soluble ascorbic acid derivative that is lipophilic. APPS has lipophilic groups and a hydrophilic group, so it forms a micelle in aqueous solution. In the body, APPS is converted into ascorbic acid, and APPS exhibits a range of bioactivities, such as having potent oxygen radical scavenging activity and preventing wrinkles (21,22). APPS is lipophilic; therefore, it penetrates the skin better than ascorbic acid. For this reason, APPS can be used in pharmaceuticals in the future.

An amphiphilic block copolymer that consists of hydrophobic and hydrophilic chains (e.g., chains of polyethylene glycol (PEG)) forms a polymeric micelle in water, allowing consistent dispersion in aqueous solution, while incorporating various poorly water-soluble drugs. A study on DDSs is examining the use of such block copolymers as nanocarriers for drug transport (23). Previous studies have reported that a polymeric micelle incorporating an anticancer agent enables exceptional drug accumulation at target sites, improved pharmacologic effects, and reduced adverse reactions (24, 25). Although most chemotherapeutic agents are low-molecular-weight compounds, high-molecular-weight micelles, produced using novel techniques, hold great promise as antitumor agents. Distearoyl phosphatidylethanolamine-PEG 2000 (DSPE-PEG 2000) is a surfactant combining a PEG chain and a phospholipid (DSPE; phospholipids are a component of biological membranes) via a negatively charged spacer (26). Ridaforolimus is a rapamycin derivative with anticancer activity. DSPE- PEG 2000 was used to prepare micelles incorporating ridaforolimus, which increased the solubility of the drug (27). In addition, DSPE-PEG 2000 has been used as a component of a nanocarrier targeting the skin, with doxorubicin is the anticancer agent. Inclusion of doxorubicin in the nanocarrier improved skin penetration of the drug (28,29).

Isopropyl myristate (IPM) is a percutaneous penetration enhancer that is most often used in local and transdermal preparations. A study has suggested that IPM is taken up by the lipid matrix of the stratum corneum, where it alters the fluidity of the lipid bilayers, but the precise mechanism has yet to be revealed (30). IPM is also used in emulsion preparations. Polyphenols are known to be antioxidants. To remedy the low level of dermal transfer of polyphenols, a microemulsion was prepared using IPM in the oil phase, and an aqueous sodium chloride solution, polyoxyethylene sorbitan monooleate (a surfactant, Tween® 80), and ethanol (as a cosurfactant) in the water phase. This microemulsion increased the solubility of a polyphenol, thus allowing increased dermal transfer (31,32).

Nadifloxacin (NDFX) has potent bactericidal activity against *Propionibacterium acnes* (*P. acnes*) and other Gram-positive and Gram-negative bacteria (33,34). It is a new, poorly water-soluble fluoroquinolone (log P of 2.47 (35)) that is widely used to topically treat multiple types of acne lesions that cause inflammation. P. acnes is a most leading bacteria of acne vulgaris and causes chronic inflammation in the pilosebaceous glands of the skin. In addition, Cytokines from host mononuclear cells and keratinocytes induce immune responses in response to P. acnes colonization. As a result, Inflammatory acne develops and worsens. Acne is mainly treated with topical therapy, oral therapy and chemical peeling. In addition, the inherent fluorescence of NDFX (36,37) is useful as an indicator of tissue penetration. So NDFX was selected as a model drug to track fluorescence and to confirm encapsulation efficiency in nanocarrier.

In the present study, APPS was applied to prepare stable nanocarriers incorporating NDFX and attempted to apply APPS having active oxygen scavenging effect as a skin-targeting DDS base material. IPM was used as an additive to promote skin permeability of nanoparticles. After synthesis, we will characterize the nanoparticles and assess their skin penetrating ability to determine their effectiveness as a nanocarrier skin-targeted drug delivery system.

MATERIALS AND METHODS

Materials

APPS was obtained from Showa Denko Co., Ltd., Japan (Fig. 1). DSPE-PEG 2000 was purchased from NOF Co., Ltd., Japan. NDFX was purchased from Sigma-Aldrich Co., Ltd., Japan. IPM and any other reagents were purchased from Wako Pure Chemical Industries, Ltd., Japan.

Preparation of Nanoparticles

APPS and IPM (1 mmol/L and 0.5 mmol/L in distilled water, respectively) were mixed, and the suspension comprising APPS/IPM = 1/0.5 (molar ratio) was sonicated for 5 min with an ultrasonic homogenizer (model NR-600 M, manufactured by Microtech-Nithion Co.). Subsequently, DSPE- PEG 2000 1 mmol/L was added to the suspension, which was sonicated again for 5 min to prepare nanoparticles. 50 μL of $MgCl_2$ solution prepared at different concentrations was added to 2 mL of the nanoparticles, and the mixture was sonicated for 3 min.

In the hydration method, various lipids are dissolved in an organic solvent and the solvent is removed using a rotary evaporator to prepare a lipid film. And, to obtain a suspension, the prepared film is hydrated with distilled water or saline (38,39). In our experiment, DSPE- PEG 2000 1 mmol/L was dissolved in methanol with NDFX 0.01 mmol/L in a pear-shaped flask. The thin-film was prepared from the dissolved sample by vacuum distillation (warm bath: 40°C). The prepared suspension of APPS/IPM = 1/0.5 (molar ratio) and the film composed of DSPE-PEG 2000/NDFX = 1/0.01 (molar ratio) were combined in the flask.

Methods

Particle Size and Zeta Potential

The average particle size and zeta potential of the nanoparticles dispersed in water were determined by dynamic light scattering (DLS) using a Zetasizer Nano ZS (Malvern Instruments, Malvern, UK). Each sample was added to a capillary cell. A measurement condition was carried out set Zero was 120 s and measurement time was 180 s.

Encapsulation Efficiency Rate (EE%)

To confirm the amount of NDFX encapsulated in the nanoparticles, NDFX was quantified. Each sample was filtered through a 0.8-μm membrane filter, centrifuged (200,000×g, 30 min, 4°C; CS 100 GXL, Hitachi Koki Co., Ltd., Japan), and the supernatant mixed 1/1 (*v*/v) with 0.01 mol/L NaOH in methanol. The resulting samples were quantified by high-performance liquid chromatography (HPLC). The percentage of total NDFX to the amount of NDFX entrapped in the nanoparticle solution was calculated as EE%.

Transmission Electron Microscopy (TEM) Observation

To evaluate the microstructure of the nanoparticles, they were characterized using a JEM-1400 Plus transmission electron microscopy (JEOL Ltd., Tokyo, Japan). Samples were adsorbed on a carbon-coated copper grid (400 mesh), negatively stained with 2% phosphotungstic acid (pH = 7.0) for 15 s, and then observed under an accelerating voltage of 80 kV.

Acquisition of ^{31}P- NMR Spectra

The structure of carrier component of the nanoparticles was determined by ^{31}P–NMR. Each sample for ^{31}P- NMR was prepared at twice the concentration as was typically prepared (i.e., APPS was 2 mmol/L, IPM was 1 mmol/L, DSPE-PEG 2000 was 2 mmol/L, and $MgCl_2$ was 25×10^{-4} mmol/L). For ^{31}P- NMR, the sample and D_2O were mixed 9:1 (*v*/v), and 85% phosphoric acid, diluted 100 times, was used as an internal standard solution. Prepared samples were measured with the Varian NMR System 400 MHz (Agilent Technologies, Inc. USA). The resonance frequency was 161.8 MHz, pulse width was 45°, relaxation time was 4.400 s, scan time was 0.600 s, temperature was 25°C, and the accumulation count was 8192 times.

Stability Study

To evaluate the stability of the prepared nanoparticles, they were stored for 14 days under a light shielding at 25°C. The particle sizes and zeta potentials were measured at predetermined time intervals (0, 1, 3, 5, 7, and 14 days).

1,1-Diphenyl-2-picryl-hydrazyl (DPPH) Radical Scavenging Assay

The DPPH radical scavenging assay was used to evaluate the antioxidant power of each sample. DPPH dissolved in methanol at 100 μmol/L and varying concentrations of samples

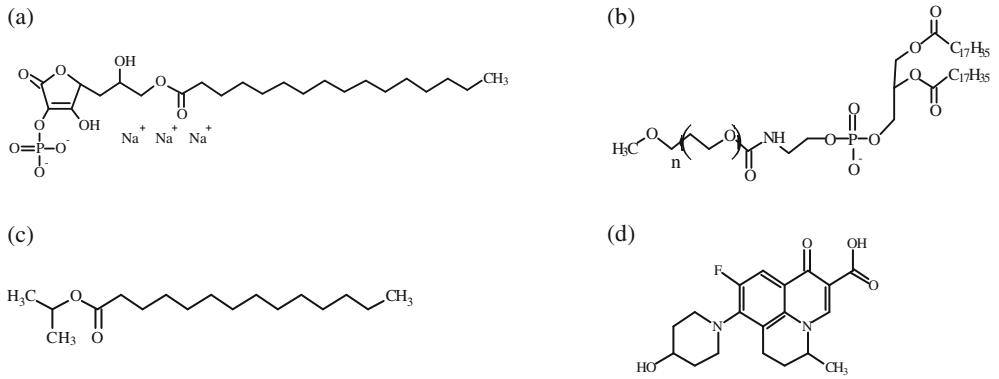

Fig. 1 Chemical structure. (**a**) Trisodium L-ascorbyl 2-phosphate 6-palmitate (APPS), (**b**) Distearoylphosphatidylethanolamine-PEG 2000 (DSPE-PEG 2000), (**c**) Isopropyl myristate (IPM), (**d**) Nadifloxacin (NDFX).

were mixed (50 μL each) in a 96-well microplate. DPPH methanolic solution with distilled water (50 μL/50 μL) and methanol with purified water (50 μL/50 μL) were used as the no nanoparticle control and blank, respectively. After setting samples in the microplate reader (SPECTRA MAX 190, Molecular Devices, Inc., USA), samples were incubated for 20 min and 37°C. The absorbance of the samples was measured at 517 nm. The inhibition rate was calculated from the obtained readings, and the 50% inhibitory concentration (IC_{50}) was determined. Data are expressed as means ± standard deviations (S.D.). Samples were evaluated by a single-step multiple comparison test of variance (*Tukey's test*).

Skin Penetration Test

To evaluate the skin permeability of NDFX, a skin penetration test was performed with the drug alone and with the equivalent amount of nanoparticle-encapsulated drug.

As pretreatment, a piece of skin of Yucatan micropigs (YMPs, females, 5 months old), which had been cryopreserved at −80°C, was thawed at 4°C for 12 h before it was used. After thawing, the subcutaneous fat was removed from the skin. The skin was cut into pieces of approximately 2.5 cm × 2.5 cm. The stratum corneum was removed from each piece of skin by tape stripping 30 times. Treated YMP skin was approximately 2–3 mm thick. Subsequently, the pretreated pieces of YMP skin were placed dermis side down on paper towels wetted with saline, and were stored at 4°C for 12 h before the skin penetration test.

Franz Cell chambers (PermeGear, Inc. USA) having ~0.95 cm^2 of effective penetration area were used for the skin penetration tests. The receiver phase was filled with ~9.5 mL of 5% albumin in saline; it was kept at 32°C and stirred during the test. A piece of the pretreated skin was set in the chamber with the epidermis against the donor phase and the dermis against the receiver phase. 2 mL of sample was applied to the donor phase, and the test was allowed to proceed for 24 h.

After completion of the test, the pieces of the skin were removed from the apparatus and washed gently. The affected area of the skin was cut into little pieces. To 0.2 g of skin pieces was added acetonitrile: 10 mmol/L NaOH (2 mL/2 mL). The mixture was homogenized at 26,000 rpm for 2 min using a POLYTRON®PT-MR2500 (Central Scientific Commerce, Inc. Japan) and centrifuged at 2600×g, 25°C for 30 min. The supernatant was collected and centrifuged at 20,000×g, 4°C for 10 min. The resultant supernatant was filtered through a 0.2 μm membrane filter, and assayed for NDFX content. The cumulative amount of transdermal NDFX in the skin of YMPs after 24 h was quantified by the HPLC method detailed in section 2.3.9.

Fluorescence Microscopy

To visualize the transfer of NDFX to the skin of YMPs, the skin sections were observed by fluorescence microscopy. After finishing the skin penetration test, the affected area was cut into pieces of approximately 7.0 cm × 2.0 mm. The pieces were put into a plastic embedding dish and covered with an embedding agent for preparing frozen tissue sections, Tissue-Tek® optimum cutting temperature (O.C.T) compound (Sakura Finetech Japan Co., Ltd., Japan). The samples were completely frozen at −80°C. Sections were made of the frozen sample at a 0.2 μm thickness. The sections were observed at an excitation wavelength of 340–390 nm using an inverted fluorescence microscope (Power IX71, Olympus Co, Japan).

HPLC Analysis

The HPLC assay to analyze the NDFX content for the encapsulation efficiency and the transdermal accumulation assays used a Shimadzu LC-20A ultraviolet visible light photometer (Shimadzu Co, Japan) and a Waters e 2795 ultraviolet visible light photometer (Japan Waters Co., Ltd., Japan), respectively. The mobile phase was water/

acetonitrile/acetic acid = 130/70/1 at a flow rate of 1.0 mL/min. The injection volume was 50 μL. The HPLC column was an Inertsil® ODS-3 column (φ5 μm, 4.6 × 150 nm, GL Sciences Inc., Japan). The UV detector wavelength was set at 280 nm. The column temperature was kept at 35°C.

RESULTS AND DISCUSSION

Initial Characterizing of APPS/DSPE-PEG 2000/IPM Nanoparticles

Size of Nanoparticles

Table I shows the particle size distribution measurements of the prepared APPS/DSPE-PEG 2000/IPM nanoparticles. The average particle diameters of APPS/DSPE-PEG 2000/IPM with compositions of 1/1/0.5, 1/1/1, and 1/1/2 were 180.8 ± 12.3, 261.3 ± 19.7, and 350.2 ± 33.0 nm, respectively. From hese results, the nanoparticle sizes tended to increase as the concentration of IPM increased. It is known that the emulsion improves the stability by miniaturization (13). APPS/DSPE-PEG 2000/IPM with ratios of 1/1/0.5 produced the smallest particle size of the prepared nanoparticles. Therefore, it was deemed appropriate for further study.

Stability of Nanoparticles

When the APPS/DSPE-PEG 2000/IPM = 1/1/0.5 nanoparticles were initially prepared, they were translucent, light blue in color, with an average particle diameter of 175.9 nm. After 24 h, they became turbid, with an average particle diameter of 355.5 nm, and therefore they were recognized to aggregate (Fig. 2). By adjusting the amount of salt, nanoparticles will resist coalescing and aggregating due to a moderate, salt-dependent repulsion occurring among the charged nanoparticles (6). Increasing concentrations of magnesium chloride ($MgCl_2$) were added to the APPS/DSPE-PEG 2000/IPM = 1/1/0.5 nanoparticles to attempt to stabilize them. To APPS, APPS/IPM = 1/0.5, and APPS/DSPE-PEG 2000/IPM = 1/1/0.5 was added 2.5×10^{-4} mmol/L $MgCl_2$. Both APPS and APPS/IPM = 1/0.5 turned cloudy (Fig. 3), but APPS/DSPE-PEG 2000/IPM = 1/1/0.5 did not. The result shows that $MgCl_2$ contributed to the stability of the nanoparticles. To confirm the effect of $MgCl_2$ on the nanoparticles, different concentrations of $MgCl_2$ were prepared and added to the APPS/DSPE-PEG 2000/IPM = 1/1/0.5, and the particle size distribution was measured. The nanoparticle size decreased with increasing concentration of $MgCl_2$ (Fig. 4). APPS/DSPE-PEG 2000/IPM = 1/1/0.5, APPS/DSPE-PEG 2000/IPM/$MgCl_2$ = 1/1/0.5/2.5×10^{-4}, APPS/DSPE-PEG 2000/IPM/$MgCl_2$ = 1/1/0.5/6.25×10^{-4}, and APPS/DSPE-PEG 2000/IPM/$MgCl_2$ = 1/1/0.5/12.5×10^{-4} produced sharp particle size distributions. APPS/DSPE-PEG 2000/IPM/$MgCl_2$ = 1/1/0.5/2.5×10^{-3} was presumed to be unstable because it appeared different than the other nanoparticles and precipitated during storing for 24 h at 25°C.

The charge on the particle surface is important for dispersibility and stability of the nanoparticle. So, each prepared sample was assayed for zeta potential (Table I). The zeta potentials of APPS and DSPE-PEG 2000 were −66.9 ± 3.5 mV and −23.9 ± 4.3 mV, respectively. Because APPS/DSPE-PEG 2000/IPM = 1/1/0.5 was measured at −67.9 ± 3.0 mV, this zeta potential was presumably derived from APPS. APPS/DSPE-PEG 2000/IPM/$MgCl_2$ = 1/1/0.5/2.5×10^{-5}, APPS/DSPE-PEG 2000/IPM/$MgCl_2$ = 1/1/0.5/6.25×10^{-5}, APPS/DSPE-PEG 2000/IPM/$MgCl_2$ = 1/1/0.5/1.25×10^{-4}, and APPS/DSPE-PEG 2000/IPM/$MgCl_2$ = 1/1/0.5/2.5×10^{-3} were measured at −61.4 ± 3.0 mV, −57.6 ± 2.3 mV, −34.6 ± 1.5 mV, and −15.3 ± 1.0 mV, respectively. The result shows that, as the concentration of $MgCl_2$ in the nanoparticles increases, the absolute value of the zeta potential decreases.

According to Singh *et al.*, nanoparticles that have a zeta potential beyond an absolute value of ~30 mV are stable in suspension, as the surface charge of particles prevents agglomeration (40). Because APPS/DSPE-PEG 2000/IPM/$MgCl_2$ = 1/1/0.5/2.5×10^{-3} had an absolute zeta potential of less than 30 mV, this nanoparticle was unstable and produced precipitates. As the concentration of $MgCl_2$ in the aqueous solution increases, the electrostatic repulsive forces due to the interaction between electric double layers around the particle surfaces decrease, and precipitation occurs from salting out.

Therefore, from the results of particle size and zeta potential measurements, it was determined that APPS/DSPE-PEG 2000/IPM/$MgCl_2$ = 1/1/0.5/12.5×10^{-4} was the most stable of the prepared nanoparticles.

Encapsulation of drug in nanoparticles

Table I shows the particle size, zeta potential, and EE% of APPS/DEPE-PEG 2000/IPM/NDFX nanoparticles. APPS/DSPE- PEG 2000/IPM/NDFX = 1/1/0.5/0.01 had an average particle diameter of 192.2 ± 8.5 nm, zeta potential of −72.9 ± 2.6 mV, and EE% of 75.7 ± 2.5%. Moreover, APPS/DSPE-PEG 2000/IPM/NDFX/$MgCl_2$ = 1/1/0.5/0.01/12.5×10^{-4} had an average particle diameter of 157.2 ± 10.1 nm, zeta potential of −43.8 ± 2.4 mV, and EE% of 76.8 ± 7.3%. As a result, NDFX was likely encapsulated in the nanoparticles because they had a larger particle size than that of APPS/DSPE-PEG 2000/IPM = 1/1/0.5 and APPS/DSPE-PEG 2000/IPM/$MgCl_2$ = 1/1/0.5/12.5×10^{-4}, the corresponding particles without NDFX encapsulation (181.8 ± 12.3 and 129.2 ± 2.6 nm, respectively). Since NDFX is a lipophilic drug, it was encapsulated in nanocarrier

Table I Mean Particle Size, Zeta Potential (ZP), Entrapment Efficiency (EE %) of Nanoparticles

Sample	Size (nm)	ZP (mV)	EE (%)
APPS	136.7 ± 8.0	−66.9 ± 3.5	–
DSPE-PEG 2000	2.8 ± 0.1	−23.9 ± 4.3	–
APPS/ DSPE-PEG 2000 = 1/ 1	5.5 ± 0.5	−28.2 ± 3.6	–
APPS/ IPM = 1/ 0.5	206.4 ± 37.2	−68.5 ± 0.8	–
DSPE-PEG 2000/ IPM = 1/ 0.5	335.0 ± 76.3	−52.1 ± 1.0	–
APPS/ DSPE-PEG 2000/ IPM = 1/ 1/ 0.5	180.8 ± 12.3	−67.9 ± 3.0	–
APPS/ DSPE-PEG 2000/ IPM = 1/ 1/ 1	261.3 ± 19.7	−79.3 ± 0.6	–
APPS/ DSPE-PEG 2000/ IPM = 1/ 1/ 2	350.2 ± 33.0	−87.4 ± 2.7	–
APPS/ DSPE-PEG 2000/ IPM/ MgCl2 = 1/ 1/ 0.5/ 2.5×10^{-4}	156.8 ± 1.4	−61.4 ± 0.7	–
APPS/ DSPE-PEG 2000/ IPM/ MgCl2 = 1/ 1/ 0.5/ 6.25×10^{-4}	141.3 ± 1.3	−57.6 ± 2.3	–
APPS/ DSPE-PEG 2000/ IPM/ MgCl2 = 1/ 1/ 0.5/ 12.5×10^{-4}	129.2 ± 2.6	−34.6 ± 1.5	–
APPS/ DSPE-PEG 2000/ IPM/ MgCl2 = 1/ 1/ 0.5/ 2.5×10^{-3}	126.4 ± 1.9	−15.3 ± 1.0	–
APPS/ DSPE-PEG 2000/ IPM/ NDFX = 1/ 1/ 0.5/ 0.01	192.2 ± 8.5	−72.9 ± 2.6	75.7 ± 2.5
APPS/ DSPE-PEG 2000/ IPM/ NDFX/ MgCl2 = 1/ 1/ 0.5/ 0.01/ 12.5×10^{-4}	157.2 ± 10.1	−43.8 ± 2.4	76.8 ± 7.3

Results are expressed as mean ± S.D. (n = 3)

by interaction with fatty chains of APPS, DSPE-PEG 2000 and IPM. In addition, the zeta potentials would not be expected to change significantly, and encapsulating NDFX would increase its dispersed stability in water.

Stability Test

Nanoparticles are thermodynamically unstable systems and the state and stability of the emulsions differ greatly due to the preparation methods and slight composition differences. Fig. 5 shows the results of the evaluation of the particles for stability in water under light-shielding at 25°C for 14 days. APPS/DSPE-PEG 2000/IPM = 1/1/0.5 and APPS/DSPE-PEG 2000/IPM/NDFX = 1/1/0.5/0.01, without added $MgCl_2$, had average particle diameters of 180.8 ± 12.3 and 192.2 ± 8.5 nm, respectively, on the first day, but increased in size over time, reaching 752.1 ± 65.6 and 673.4 ± 196.9 nm, respectively, by day 14. In contrast, nanoparticles with added $MgCl_2$, APPS/DSPE-PEG 2000/IPM/$MgCl_2$ = 1/1/0.5/12.5×10^{-4} and APPS/DSPE-PEG 2000/IPM/NDFX/$MgCl_2$ = 1/1/0.5/0.01/12.5×10^{-4}, had average particle diameters of 129.2 ± 2.6 and 157.2 ± 10.1 nm on the first day, but 144.9 ± 6.2 and 182.2 ± 7.3 nm by day 14, respectively. Since the particle size did not change significantly, it was concluded that the nanoparticles existed stably in water.

The inorganic salt may be useful when the dispersoid can be stabilized by changing the hydration state of the hydrophilic group of the amphipathic molecule (41). This imparts three effects to the emulsion. First, particle size

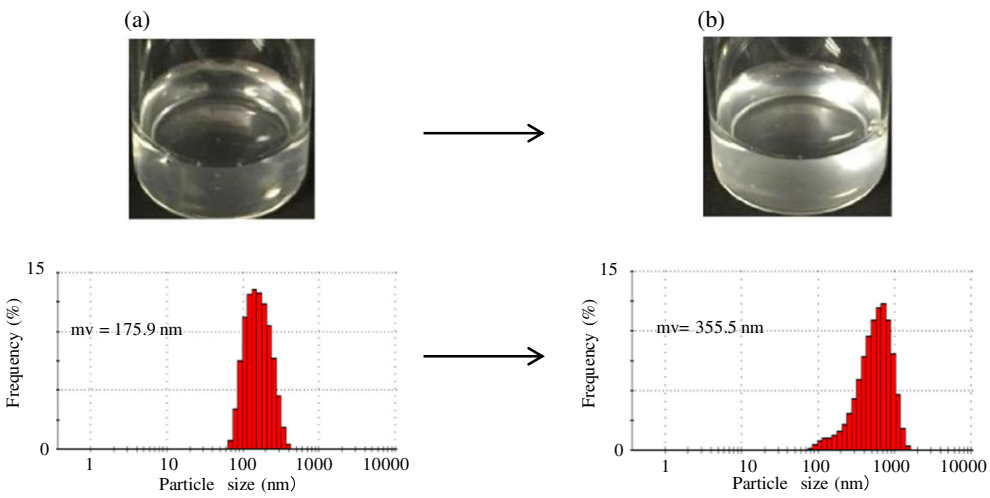

Fig. 2 Changes in particle size of APPS/DSPE-PEG2000/IPM = 1/1/0.5 nanoparticles after 24 h at 25°C. (**a**) Nanoparticles after preparation, (**b**) Nanoparticles after 24 h.

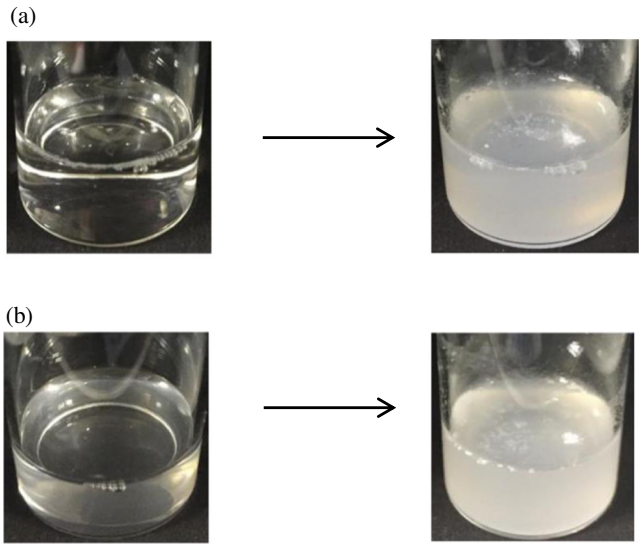

Fig. 3 Effect of $MgCl_2$ solution on the particle. (**a**) APPS, (**b**) APPS/IPM = 1/0.5.

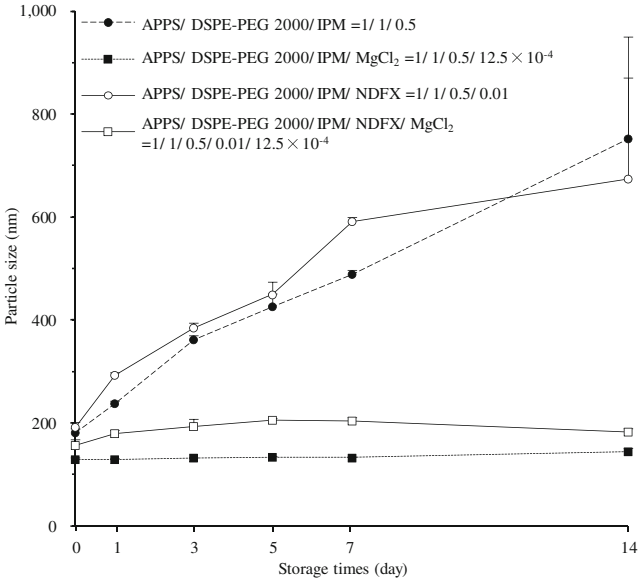

Fig. 5 Changes in particle size of APPS/DSPE-PEG 2000/IPM = 1/1/0.5 nanoparticles and APPS/DSPE-PEG 2000/IPM/NDFX = 1/1/0.5/0.01 nanoparticles after the storage at 25°C. Each point represents the mean ± S.D. (n = 3).

decreases. Second, collision frequency decreases due to the increased attraction between particles based on Van der Waals interactions. Finally, the surfactant increases adsorption density (42,43).

In this study, adding $MgCl_2$ to the system decreased particle size compared to that without $MgCl_2$ (Table I), and we observed a sharp particle size distribution on the first day of the stability test. Furthermore, with $MgCl_2$, we were not able to see significant changes in particle diameter when the nanoparticles were stored for 14 days. These properties resulted from the three aforementioned effects of the inorganic salt.

Fig. 4 Effect of concentration of $MgCl_2$ solution on the particle size. Results are expressed as mean ± S.D. (*n* = 3).

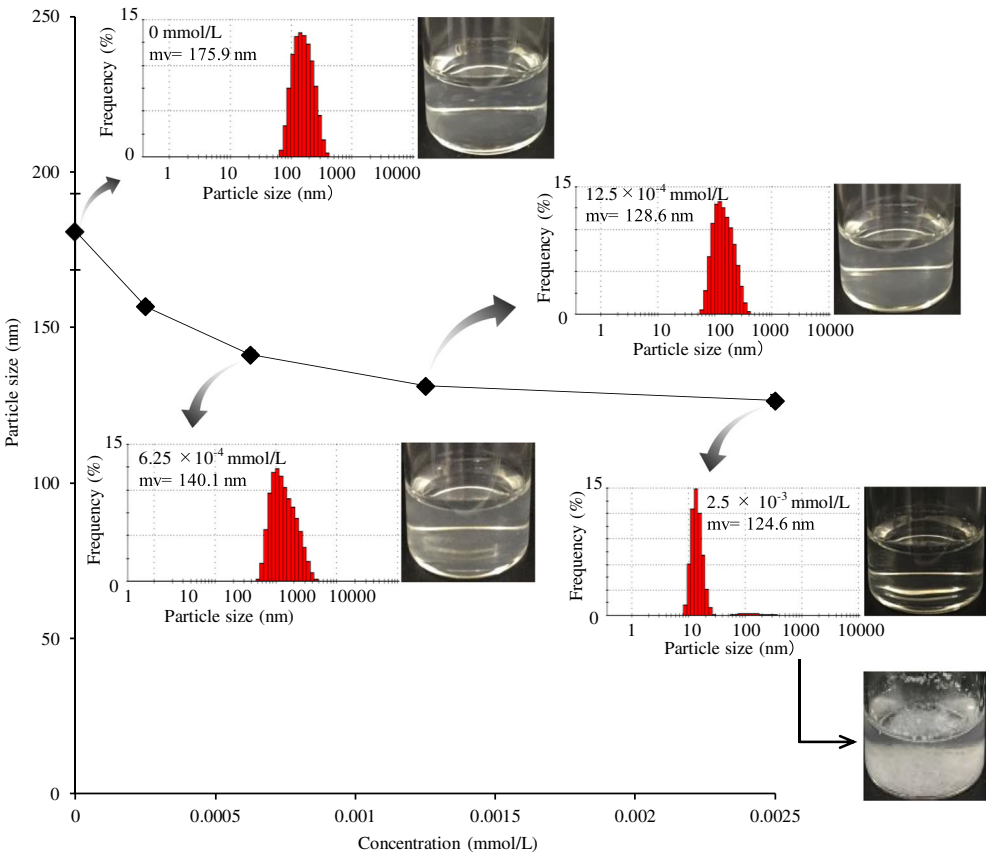

In terms of zeta potential, by the results of the stability test, APPS/DSPE-PEG 2000/IPM = 1/1/0.5 and APPS/DSPE-PEG 2000/IPM/NDFX = 1/1/0.5/0.01 were −88.9 and −76.2 mV, respectively on the first day. After 14 days, they were −44.3 and −40.9 mV, respectively, and their zeta potentials were rising. Thus, a zeta potential of approximately −70 mV increases collision frequency between particles and induces aggregation and collapse of nanoparticles. Additionally, the zeta potentials converged to about −40 mV at 14 days because the particle sizes became enlarged by aggregation and collapse. In contrast, APPS/DSPE-PEG 2000/IPM/$MgCl_2$ = 1/1/0.5/12.5×10^{-4} and APPS/DSPE-PEG 2000/IPM/NDFX/$MgCl_2$ = 1/1/0.5/$0.01/12.5 \times 10^{-4}$ were −44.4 and −44.1 mV, respectively, on the first day, but −31.2 and −43.0 mV, respectively, by day 14. The zeta potential was maintained at approximately -(30~40) mV for 14 days. Accordingly, the prepared nanoparticles could disperse stably in water at approximately −40 mV.

Shape Evaluation of APPS/DSPE-PEG 2000/IPM/NDFX Nanoparticles

Figure 6 shows the TEM results for the nanoparticles. The TEM results conformed to the results of the particle size measurements, so that they appeared to be ~100–200 nm wide. DSPE-PEG 2000 forms micelles with lipid membrane and disk structures (44, 45). APPS/DSPE-PEG 2000/IPM/NDFX nanoparticles were likely to form either structure. Generally, double membrane structures, such as liposomes, form lamellar structures (46). We did not observe lamellar structures in the TEM images of our prepared nanoparticles, so they were micellar. In addition, even if NDFX was encapsulated inside APPS/DSPE-PEG 2000/IPM = 1/1/0.5, the nanoparticles were able to maintain their shape.

Structural Evaluation of APPS/DSPE-PEG 2000/IPM Nanoparticles

^{31}P–NMR

^{31}P–NMR is widely used to characterize the configuration of the structure of phospholipids. Thus, evaluating the atomic state of phosphorus allowed us to determine the change of the molecular state of APPS and DSPE-PEG 2000 in the nanoparticle (39,47). Figure 7 shows the results of the ^{31}P–NMR. APPS alone produced a shift at 1.42 ppm ($v_{1/2}$ = 3.3 Hz) and was confirmed to have high mobility (Fig. 7(a)). DSPE-PEG 2000 alone produced a shift at −0.23 ppm ($v_{1/2}$ = 20.4 Hz) (Fig. 7(b)). The peak was broad because DSPE-PEG 2000 was a surfactant and had viscosity. APPS/IPM = 1/0.5 produced a shift at 1.42 ppm ($v_{1/2}$ = 3.0 Hz); the peak width became narrower, with a greater mobility of phosphorus compared with that of APPS alone (Fig. 7(c)). This was presumed to arise from the high mobility of IPM (48). APPS/DSPE-PEG 2000 = 1/1 produced two shifts, 1.47 ppm ($v_{1/2}$ = 5.0 Hz) and −0.13 ppm ($v_{1/2}$ = 8.0 Hz) (Fig. 7(d)). The chemical shift at 1.47 ppm ($v_{1/2}$ = 5.0 Hz) arose from the APPS. The mobility of phosphorus was reduced because the peak shifted to the lower field side and broadened compared with that of APPS alone. However, the shift at −0.13 ppm ($v_{1/2}$ = 8.0 Hz) arose from DSPE-PEG 2000. Intermolecular interaction occurred between APPS and DSPE-PEG 2000 because the peak shifted to the lower field side compared with that of DSPE-PEG 2000 alone. Besides, ^{31}P–NMR is used to distinguish PEGylated micelles or liposomes. Micelles show narrow peak widths and liposomes show wide peak widths in ^{31}P–NMR (49). It was inferred from the peak derived from the DSPE-PEG 2000 of APPS/DSPE-PEG 2000 = 1/1 that APPS/DSPE-PEG 2000 = 1/1 forms micelles to produce a narrow peak width. APPS/DSPE-PEG2000/IPM = 1/1/0.5 produced two shifts, 1.51 ppm ($v_{1/2}$ = 5.2 Hz) and −0.13 ppm ($v_{1/2}$ = 8.7 Hz) (Fig. 7(e)). The chemical shift at 1.51 ppm ($v_{1/2}$ = 5.2 Hz) arose from APPS. It was assumed that the mobility of phosphorus was reduced because the peak shifted to the lower field side and became broad compared with that of APPS alone and APPS/DSPE-PEG 2000 = 1/1. The shift at −0.13 ppm ($v_{1/2}$ = 8.7 Hz) was on the lower field side compared with that of DSPE-PEG 2000 alone. So, it seems that PEG has intermolecular interactions with APPS and IPM. Additionally, the narrow peak widths suggest the formation of micelles. APPS/DSPE-PEG2000/IPM = 1/1/0.5 has been confirmed already to have micelle-like particles by TEM (Fig. 6). Hence, the prepared nanoparticles were likely to have formed micelles. It was difficult to measure APPS/DSPE-PEG 2000/IPM/$MgCl_2$ = 1/1/0.5/12.5×10^{-4} using ^{31}P–NMR because of the interference from the paramagnetic Mg^{2+} ion (Fig. 7(f)) (50). Therefore, after nanoparticle preparation, the phosphorus of APPS and DSPE-PEG 2000 seemed to suppress the mobility due to hydrophobic interactions among the hydrophobic chains of APPS, DSPE-PEG 2000, and IPM.

Functional Evaluation of Nanoparticles

DPPH Radical Scavenging Activity Assay

Because APPS has antioxidant activity (22), APPS/DSPE-PEG 2000/IPM/NDFX nanoparticles are expected to have a similar effect when applied to the skin. The DPPH radical scavenging activity assay was used to evaluate the antioxidant activity of APPS, APPS/DSPE-PEG 2000/IPM/NDFX = 1/1/0.5/0.01 and APPS/DSPE-PEG 2000/IPM/NDFX/$MgCl_2$ = 1/1/0.5/0.01/12.5×10^{-4}.

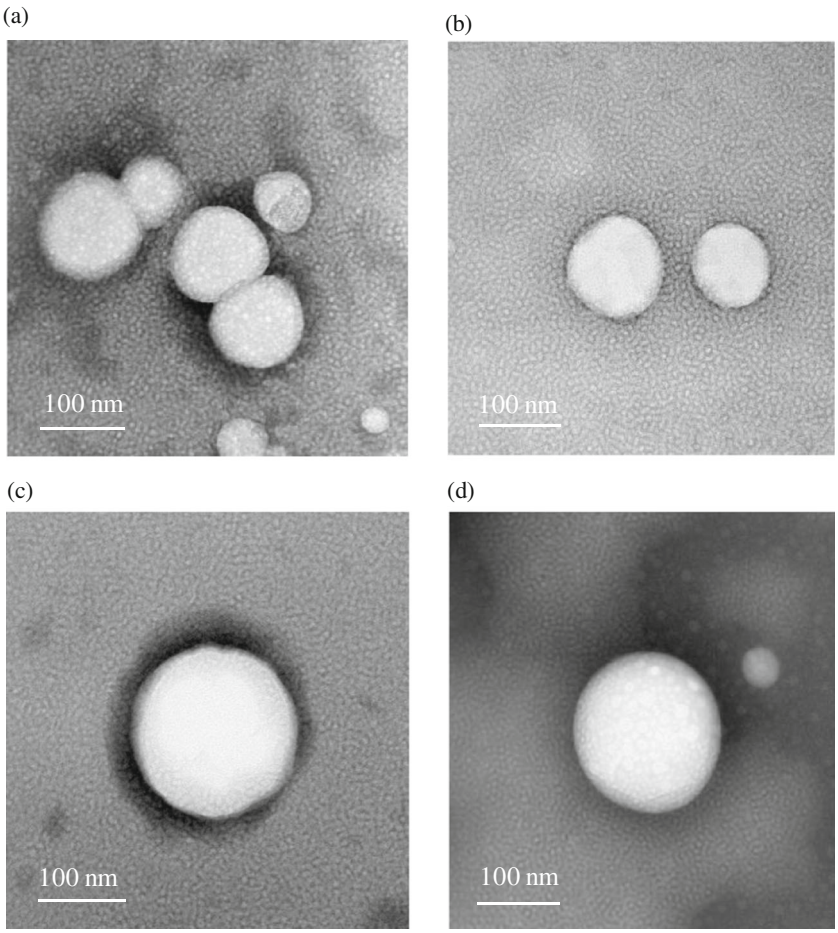

Fig. 6 TEM image of nanoparticles. (**a**) APPS/DSPE-PEG 2000/IPM = 1/1/0.5, (**b**) APPS/DSPE-PEG 2000/IPM/$MgCl_2$ = 1/1/0.5/12.5 × 10^{-4}, (**c**) APPS/DSPE-PEG 2000/IPM/NDFX = 1/1/0.5/0.01, (**d**) APPS/DSPE-PEG 2000/IPM/NDFX/$MgCl_2$ = 1/1/0.5/0.01/12.5 × 10^{-4}.

Figure 8 shows the results of the assay. The IC_{50} of APPS, APPS/DSPE-PEG 2000/IPM/NDFX = 1/1/0.5/0.01 and APPS/DSPE-PEG 2000/IPM/NDFX/$MgCl_2$ = 1/1/0.5/0.01/12.5 × 10^{-4} were 38.0 ± 3.9, 37.1 ± 2.1, and 37.6 ± 1.3 μmol/L, respectively. This confirmed that the antioxidant activity of APPS was not lost after preparation of the nanoparticles. In consequence, the nanoparticles are expected to act, not only as carriers that encapsulate poorly water-soluble drugs or substances to protect them from oxidation, but also as antioxidants when used on the skin.

Skin penetration test and Fluorescence microscopy study

First, Tables II and III show the results of the skin permeation test after 24 h. NDFX was not detected in the YMP skin when NDFX suspension was tested. In contrast, the amount of NDFX found in the skin with APPS/DSPE-PEG 2000/IPM/NDFX = 1/1/0.5/0.01 and APPS/DSPE-PEG 2000/IPM/NDFX/$MgCl_2$ = 1/1/0.5/0.01:12.5 × 10^{-4} was 0.32 ± 0.17 μg/cm^2 and 0.36 ± 0.17 μg/cm^2, respectively. As a result, it was confirmed that NDFX remained in the skin with the nanoparticle formulations. Moreover, considering the EE% of NDFX into the nanoparticles, the penetration rate into the skin of APPS/DSPE-PEG 2000/IPM/NDFX = 1/1/0.5/0.01 and APPS/DSPE-PEG 2000/IPM/NDFX/$MgCl_2$ = 1/1/0.5/0.01/12.5 × 10^{-4} was 12.5 ± 5.2% and 12.1 ± 6.2%, respectively. Therefore, this suggests that the nanoparticle formulation is an effective method for delivering NDFX into the skin.

Second, Fig. 9 shows the results of observing the frozen sections of YMP skin after the skin penetration test by fluorescence microscopy. Skin treated with NDFX suspension fluoresced at its surface, but did not fluoresce underneath. This corroborates the inability to detect NDFX in the skin by the penetration test. In contrast, skin treated with APPS/DSPE-PEG 2000/IPM/NDFX = 1/1/0.5/0.01 and APPS/DSPE-PEG 2000/IPM/NDFX/$MgCl_2$ = 1/1/0.5/0.01/12.5 × 10^{-4} fluoresced brightly, especially the skin surface layer and interspace.

Scheme 1 shows the proposed skin penetration pathways of NDFX. The pathways are classified into two types. One is the stratum corneum pathway via intercellular and intracellular cornified cells, and the other is the transappendageal pathway via hair follicles and sweat glands. The stratum corneum

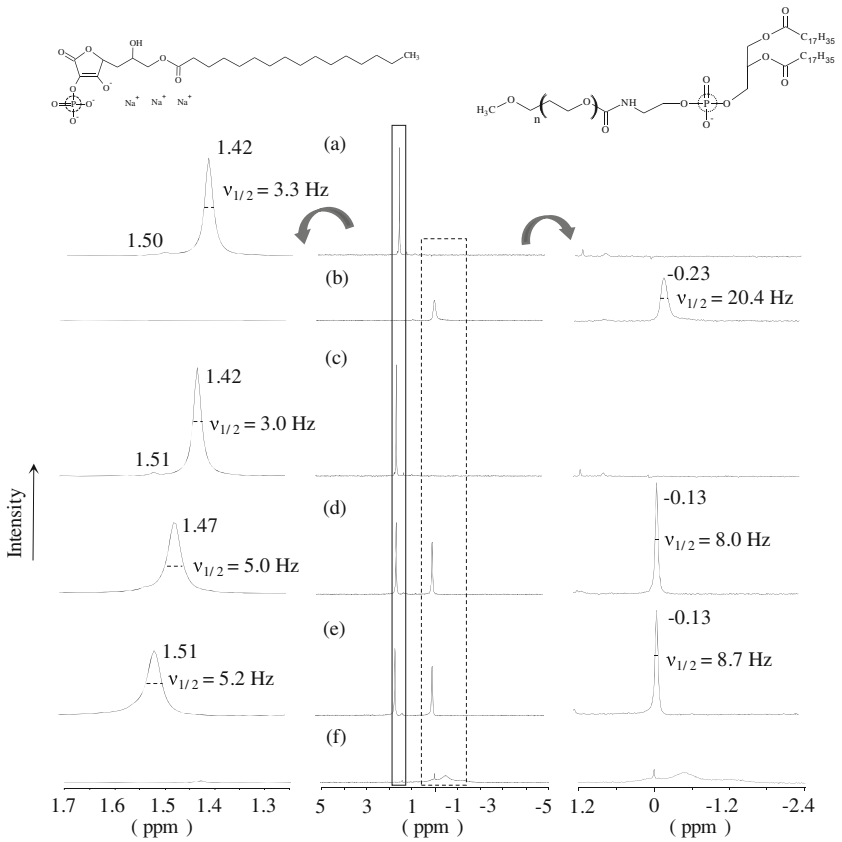

Fig. 7 ^{31}P -NMR spectra of nanoparticles. (**a**) APPS, (**b**) DSPE-PEG 2000, (**c**) APPS/IPM = 1/0.5, (**d**) APPS/DSPE-PEG 2000 = 1/1, (**e**) APPS/DSPE-PEG 2000/IPM = 1/1/0.5, (**f**) APPS/DSPE-PEG 2000/IPM/MgCl2 = 1/1/0.5/ 12.5×10^{-4}.

pathway consists mostly of the skin penetration area. Most drugs are transdermally absorbed through the intercellular pathway because the intercellular gaps have hydrophilic and hydrophobic components. Lipophilic substances have a high affinity with the constituents of the intercellular gap, so the intercellular pathway is the main penetration pathway for low molecular weight lipid soluble substances. By contrast, the transappendageal pathway represents only ~0.1% of the total skin area. However, it is used as an intradermal invasion pathway for substances with extremely low keratolytic permeability, polymers, and water-soluble substances (51). APPS/DSPE-PEG 2000/IPM/NDFX = 1/1/0.5/0.01 and APPS/DSPE-PEG 2000/IPM/NDFX/$MgCl_2$ = 1/1/0.5/ $0.01/12.5 \times 10^{-4}$ fluoresced strongly at intercellular gaps (white arrow in Fig. 9), so that NDFX used the intercellular pathway as a main skin penetration pathway.

Furthermore, "the 500 Da (Da) rule" should be considered for skin penetration of a drug. According to Bos and Meinardi, poorly water-soluble drugs and drugs with molecular weights of < 500 can be delivered to skin tissue

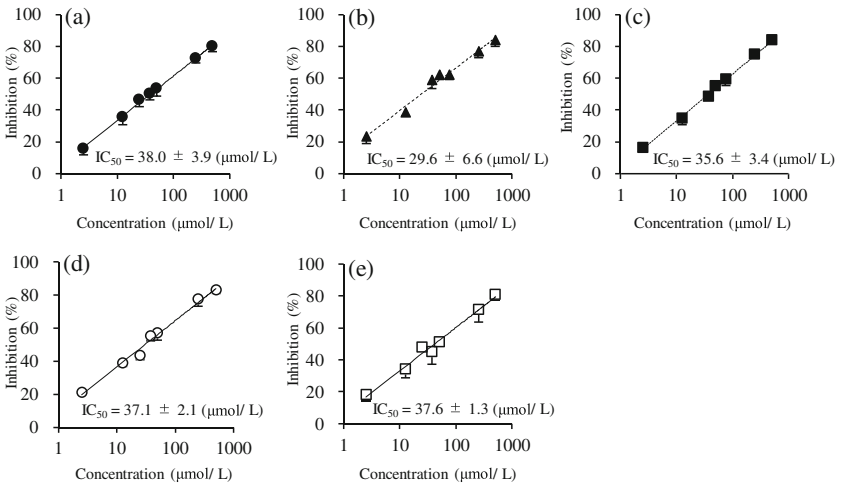

Fig. 8 Scavenging of DPPH radical by APPS. (**a**) APPS, (**b**) APPS/DSPE-PEG 2000/IPM = 1/1/0.5, (**c**) APPS/DSPE-PEG 2000/IPM/ $MgCl_2$ = 1/1/0.5/12.5 × 10^{-4}, (**d**) APPS/DSPE-PEG 2000/IPM/ NDFX = 1/1/0.5/0.01, (**e**) APPS/DSPE-PEG 2000/IPM/ $MgCl_2$/ NDFX = 1/1/0.5/0.01/ 12.5 × 10^{-4}. Results are expressed as means ± S.D. (n = 3), No significant difference (Tukey's test).

Table II Cumulative Amount of Transdermal NDFX After 24 h

Sample	Amount of trasdermal NDFX (μg/cm2)
NDFX suspension	Not detected
IPM/NDFX = 0.5/0.01	0.20 ± 0.04
APPS/DSPE-PEG 2000/IPM/NDFX = 1/1/0.5/0.01	0.32 ± 0.17
APPS/DSPE-PEG 2000/IPM/NDFX/MgCl2 = 1/1/0.5/0.01/12.5 × 10^{-4}	0.36 ± 0.17

Results are expressed as mean ± S.D. (n = 3), No significant difference (*Tukey's test*)

for the purpose of topical or systemic action without using transdermal absorption promoting technology (52). Additionally, Bouwsta surmised that liposomes functioned as a carrier delivering the drug deeply into the skin or as an absorption enhancer perturbing the structure of the stratum corneum. She believed that the liposome penetrated mainly though intercellular gaps, that there was a channel among intercellular gaps to easily pass topically applied compounds, and that the drug would penetrate through this site (53,54).

By the 500 Da rule, it is unlikely that nanoparticles would penetrate the skin, while maintaining their form. IPM, a component of our nanoparticles, is known to be a skin penetration enhancer (55). Therefore, IPM was likely involved to a large extent with NDFX penetrating the skin. When IPM/NDFX = 0.5/0.01 was subjected to the skin penetration test, NDFX remained in the YMP skin at 0.20 ± 0.04 μg/cm^2 (Table II). There was no significant difference between the nanoparticle formulations, IPM/NDFX = 0.5/0.01 and APPS/DSPE-PEG 2000/IPM/NDFX = 1/1/0.5/0.01. However, the formulations tended to accumulate larger amounts of transdermal NDFX than the IPM/NDFX = 0.5/0.01. In the fluorescence microscope images, IPM/NDFX = 0.5/0.01 had strong fluorescence at the skin surface layer and fluorescence topically in the skin. However, IPM/NDFX = 0.5/0.01 fluoresced lesser than the nanoparticle formulation in whole skin (Fig. 9). As a result, it was effective to include IPM in the skin targeting formulation, and the nanoparticle formulation was an effective means to deliver the drug effectively into the skin. Fatty acids with carbon numbers of 10–18 are endogenous components of human skin, and can enhance transdermal penetration of lipophilic and hydrophilic substances (30). APPS could produce an equivalent effect as IPM because the former contains palmitic acid, with a carbon number of 16. Furthermore, DSPE-PEG 2000 is a surfactant. Hence, the most reasonable skin permeation mechanism of NDFX is that NDFX penetrates the skin by APPS/DSPE-PEG 2000/IPM = 1/1/0.5, which consists of components with high affinity for the lipid portions of the skin, exchanging skin lipid with these lipid substances, fusing with the skin lipid, and upsetting the fluidity of the skin lipid matrix.

CONCLUSION

It was possible to form nanoparticles composed of APPS, DSPE-PEG 2000, and IPM using an ultrasonic homogenizer; from the results of the particle size distribution measurements, NDFX was encapsulated in the nanoparticles by the hydration method.

In addition, the particle size of APPS/DSPE-PEG 2000/IPM/NDFX = 1/1/0.5/0.01 increased over several days by aggregation, but APPS/DSPE-PEG 2000/IPM/NDFX/$MgCl_2$ = 1/1/0.5/0.01/12.5 × 10^{-4}, with added $MgCl_2$, could disperse stably at 25°C for at least 14 days.

By TEM observation, APPS/DSPE-PEG 2000/IPM/NDFX = 1/1/0.5/0.01 and APPS/DSPE-PEG 2000/IPM/NDFX/$MgCl_2$ = 1/1/0.5/0.01/12.5 × 10^{-4} appeared as spherical, micellar particles. Even with NDFX enclosed in APPS/DSPE-PEG 2000/IPM = 1/1/0.5, the nanoparticles were able to keep their shape. Similarly, the results of ^{31}P–NMR suggested that the prepared nanoparticles were micelles.

Both APPS/DSPE-PEG 2000/IPM/NDFX = 1/1/0.5/0.01 and APPS/DSPE-PEG 2000/IPM/NDFX/$MgCl_2$ = 1/1/0.5/0.01/12.5 × 10^{-4} have similar antioxidant activity to that of APPS. Therefore, nanoparticles could be expected to have antioxidant activity when used on the skin.

From the skin permeation test, NDFX transfer into the skin was improved by the nanoparticle formulation.

Table III Skin Retention Rate of NDFX

Sample	Skin retention of NDFX (%)
NDFX suspension	Not detected
APPS/DSPE-PEG 2000/IPM/NDFX = 1/1/0.5/0.01	12.5 ± 5.2
APPS/DSPE-PEG 2000/IPM/NDFX/MgCl2 = 1/1/0.5/0.01/12.5 × 10^{-4}	12.1 ± 6.2

Results are expressed as mean ± S.D. (n = 3)

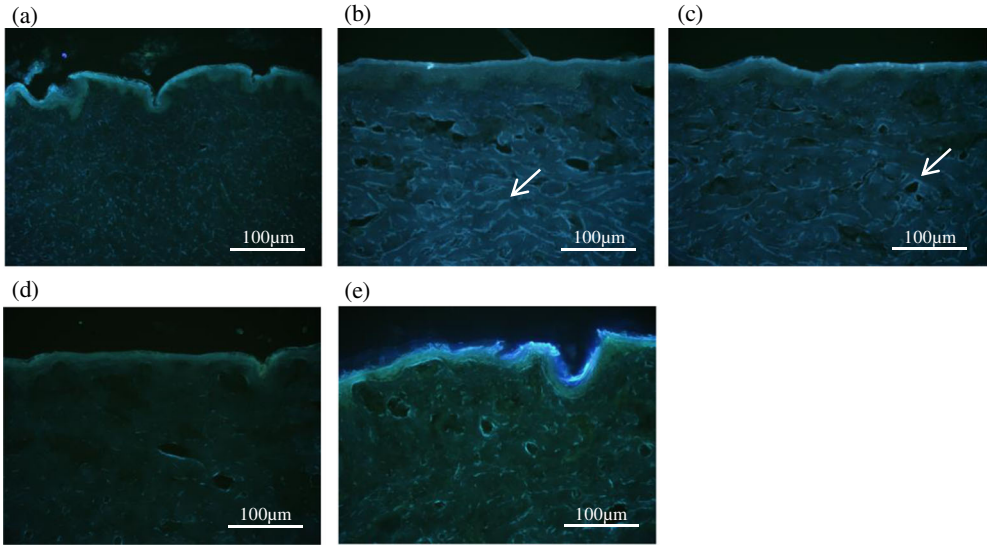

Fig. 9 Fluorescence microscope images of the epidermal side of YMP skin. (**a**) NDFX suspension, (**b**) APPS/DSPE-PEG2000/IPM/NDFX = 1/1/0.5/0.01, (**c**) APPS/DSPE-PEG2000/IPM/NDFX/$MgCl_2$ = 1/1/0.5/0.01/12.5 × 10^{-4}, (**d**) Untreated, (**e**) IPM/NDFX = 0.5/0.01.

NDFX, a model drug, is commercially available in Japan as ointment, cream, and lotion formulations. If the prepared formulations in this study become usable as a prescription design product, they will demonstrate not only the bactericidal effects of NDFX but also the antioxidant effects of the ascorbic acid of APPS. As a result, this is presumably expected to contribute to the improvement of acne lesion skin, providing a more effective treatment.

Scheme 1 The model mechanisms of action of nanoparticles as skin drug delivery systems.

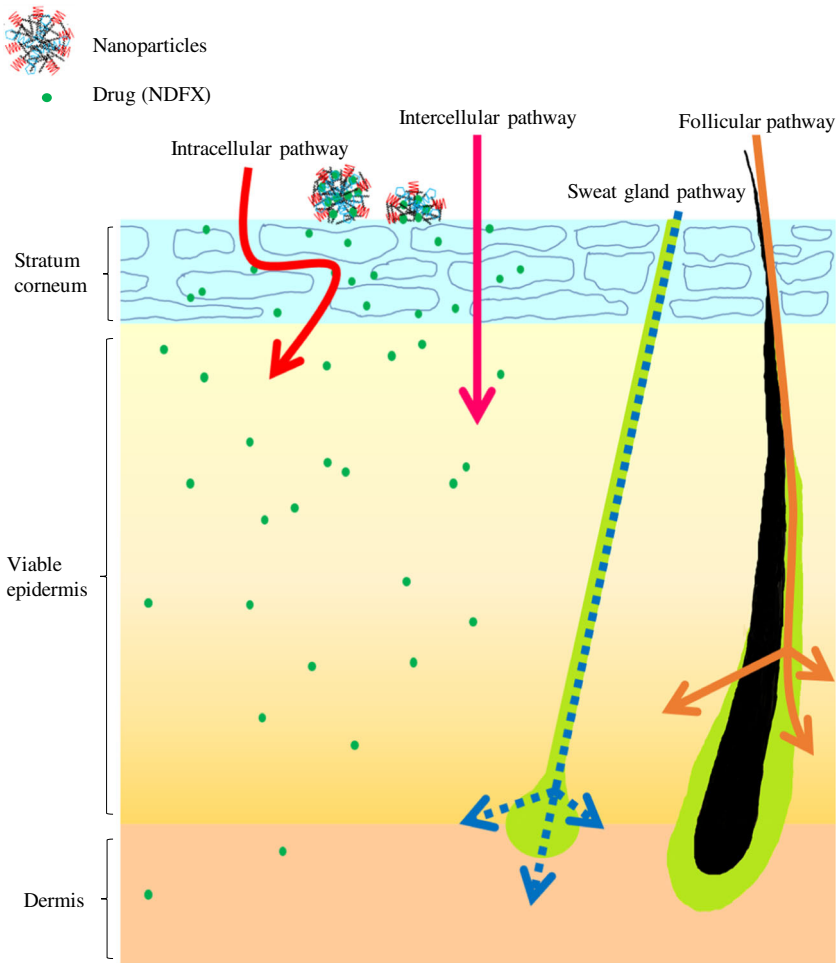

Therefore, it is suggested that nanoparticles using APPS are useful skin targeting nanocarriers.

ACKNOWLEDGMENTS AND DISCLOSURES. The authors express their appreciation to Tokai Electron Microscopy, Inc., Japan, which performed the TEM studies for this research. The authors declare that there are no conflicts of interest regarding the publication of this paper.

REFERENCES

1. Kumari A, Yadav SK, Yadav SC. Biodegradable polymeric nanoparticles based drug delivery systems. Colloids Surf B: Biointerfaces. 2010;75(1):1–18.
2. Naahidi S, Jafari M, Edalat F, Raymond K, Khademhosseini A, Chen P. Biocompatibility of engineered nanoparticles for drug delivery. J Control Release. 2013;166(2):182–94.
3. Danhier F, Ansorena E, Silva JM, Coco R, Le Breton A, Préat V. PLGA-based nanoparticles: An overview of biomedical applications. J Control Release. 2012;161(2):505–22.
4. Zhang L, Li Y, Yu JC. Chemical modification of inorganic nanostructures for targeted and controlled drug delivery in cancer treatment. J Mater Chem B. 2014;2(5):452–70.
5. Chen H, Khemtong C, Yang X, Chang X, Gao J. Nanonization strategies for poorly water-soluble drugs. Drug Discov Today. 2011;16(7–8):354–60.
6. Fryd MM, Mason TG. Advanced Nanoemulsions. Annu Rev Phys Chem. 2012;63(1):493–518.
7. Lohani A, Verma A, Joshi H, Yadav N, Karki N. Nanotechnology-based cosmeceuticals. ISRN Dermatol. 2014;843687. https://doi.org/10.1155/2014/843687.
8. Musa SH, Basri M, Masoumi HRF, Shamsudin N, Salim N. Enhancement of physicochemical properties of nanocolloidal carrier loaded with cyclosporine for topical treatment of psoriasis: In vitro diffusion and in vivo hydrating action. Int J Nanomedicine. 2017;12:2427–41.
9. Ghate VM, Lewis SA, Prabhu P, Dubey A, Patel N. Nanostructured lipid carriers for the topical delivery of tretinoin. Eur J Pharm Biopharm. 2016;108:253–61.
10. Monge-Fuentes V, Muehlmann LA, Longo JPF, Silva JR, Fascineli ML, Azevedo RB, et al. Photodynamic therapy mediated by acai oil (Euterpe oleracea Martius) in nanoemulsion: A potential treatment for melanoma. J Photochem Photobiol B Biol. 2017;166:301–10.
11. Pepe D, Carvalho VFM, McCall M, De Lemos DP, Lopes LB. Transportan in nanocarriers improves skin localization and antitumor activity of paclitaxel. Int J Nanomedicine. 2016;11:2009–19.
12. Guo F, Wang J, Ma M, Tan F, Li N. Skin targeted lipid vesicles as novel nano-carrier of ketoconazole: characterization, in vitro and in vivo evaluation. J Mater Sci Mater Med. 2015;26(4):175.
13. Qian C, McClements DJ. Formation of nanoemulsions stabilized by model food-grade emulsifiers using high-pressure homogenization: Factors affecting particle size. Food Hydrocoll. 2011;25(5):1000–8.
14. Anarjan N, Nehdi IA, Tan CP. Protection of astaxanthin in astaxanthin nanodispersions using additional antioxidants. Molecules. 2013;18(7):7699–710.
15. Takebayashi J, Tai A, Gohda E, Yamamoto I. Characterization of the radical-scavenging reaction of 2-O-substituted ascorbic acid derivatives, AA-2G, AA-2P, and AA-2S: a kinetic and stoichiometric study. Biol Pharm Bull. 2006;29(4):766–71.
16. Elmore AR. Final report of the safety assessment of L-Ascorbic Acid, Calcium Ascorbate, Magnesium Ascorbate, Magnesium Ascorbyl Phosphate, Sodium Ascorbate, and Sodium Ascorbyl Phosphate as used in cosmetics. Int J Toxicol. 2005;24(2):51–111.
17. Fočo A, Gašperlin M, Kristl J. Investigation of liposomes as carriers of sodium ascorbyl phosphate for cutaneous photoprotection. Int J Pharm. 2005;291(1–2):21–9.
18. Inoue Y, Yoshimura S, Tozuka Y, Moribe K, Kumamoto T, Ishikawa T, et al. Application of ascorbic acid 2-glucoside as a solubilizing agent for clarithromycin: Solubilization and nanoparticle formation. Int J Pharm. 2007;331(1):38–45.
19. Yoksan R, Jirawutthiwongchai J, Arpo K. Encapsulation of ascorbyl palmitate in chitosan nanoparticles by oil-in-water emulsion and ionic gelation processes. Colloids Surf B: Biointerfaces. 2010;76(1):292–7.
20. Gopinath D, Ravi D, Rao BR, Apte SS, Renuka D, Rambhau D. Ascorbyl palmitate vesicles (Aspasomes): Formation, characterization and applications. Int J Pharm. 2004;271(1–2):95–113.
21. Du CB, Liu JW, Su W, Ren YH, Wei DZ. The protective effect of ascorbic acid derivative on PC12 cells: involvement of its ROS scavenging ability. Life Sci. 2003;74(6):771–80.
22. Murakami K, Inagaki J, Saito M, Ikeda Y, Tsuda C, Noda Y, et al. Skin atrophy in cytoplasmic SOD-deficient mice and its complete recovery using a vitamin C derivative. Biochem Biophys Res Commun. 2009;382(2):457–61.
23. Yokosawa M, Sonoda Y, Sugiyama S, Saito R, Yamashita Y, Nishihara M, et al. Convection-enhanced delivery of a synthetic retinoid Am80, loaded into polymeric micelles, prolongs the survival of rats bearing intracranial glioblastoma xenografts. Tohoku J Exp Med. 2010;221:257–64.
24. Kuroda JI, Kuratsu JI, Yasunaga M, Koga Y, Saito Y, Matsumura Y. Potent antitumor effect of SN-38-incorporating polymeric micelle, NK012, against malignant glioma. Int J Cancer. 2009;124(11):2505–11.
25. Gong J, Chen M, Zheng Y, Wang S, Wang Y. Polymeric micelles drug delivery system in oncology. J Control Release. 2012;159(3):312–23.
26. Lukyanov AN, Torchilin VP. Micelles from lipid derivatives of water-soluble polymers as delivery systems for poorly soluble drugs. Adv Drug Deliv Rev. 2004;56(9):1273–89.
27. Remsberg CM, Zhao Y, Takemoto JK, Bertram RM, Davies NM, Forrest ML. Pharmacokinetic evaluation of a DSPE-PEG2000 micellar formulation of ridaforolimus in rat. Pharmaceutics. 2013;5(1):81–93.
28. Park H, Lee J, Jeong S, Im BN, Kim MK, Yang SG, et al. Lipase-Sensitive Transfersomes Based on Photosensitizer/ Polymerizable Lipid Conjugate for Selective Antimicrobial Photodynamic Therapy of Acne. Adv Healthc Mater. 2016;5(24):3139–47.
29. Boakye CHA, Patel K, Singh M. Doxorubicin liposomes as an investigative model to study the skin permeation of nanocarriers. Int J Pharm. 2015;489(1–2):106–16.
30. Tuntiyasawasdikul S, Limpongsa E, Jaipakdee N, Sripanidkulchai B. Transdermal permeation of Kaempferia parviflora methoxyflavones from isopropyl myristate-based vehicles. AAPS Pharm Sci Tech. 2014;15(4):947–55.
31. Kitagawa S, Tanaka Y, Tanaka M, Endo K, Yoshii A. Enhanced skin delivery of quercetin by microemulsion. J Pharm Pharmacol. 2009;61(7):855–60.
32. Kitagawa S, Inoue K, Teraoka R, Morita S. Enhanced skin delivery of genistein and other two isoflavones by microemulsion and prevention against UV irradiation-induced erythema formation. Chem Pharm Bull (Tokyo). 2010;58(3):398–401.
33. Kuwahara K, Kitazawa T, Kitagaki H, Tsukamoto T, Kikuchi M. Nadifloxacin, an antiacne quinolone antimicrobial, inhibits the production of proinflammatory cytokines by human peripheral blood

mononuclear cells and normal human keratinocytes. J Dermatol Sci. 2005;38(1):47–55.
34. Inoue Y, Shimura A, Horage M, Maeda R, Murata I, Sugino M, et al. Effects of the properties of creams on skin penetration. Int J Pharm. 2015;5(3):645–54.
35. Shinde U, Pokharkar S, Modani S. Design and evaluation of microemulsion gel system of nadifloxacin. Indian J Pharm Sci. 2012;74(3):237–47.
36. Inoue Y, Matsumoto M, Kimura M, Tanaka T, Kanamoto I. Comparison of the properties of brand-name and generic nadifloxacin creams. Medicina (B Aires). 2011;47(11):616–22.
37. Yang R, Fu Y, Di Li L, Liu JM. Medium effects on fluorescence of ciprofloxacin hydrochloride. Spectrochim Acta - Part A Mol Biomol Spectrosc. 2003;59(12):2723–32.
38. Moribe K, Maruyama S, Inoue Y, Suzuki T, Fukami T, Tomono K, et al. Ascorbyl dipalmitate/PEG-lipid nanoparticles as a novel carrier for hydrophobic drugs. Int J Pharm. 2010;387(1–2):236–43.
39. Moribe K, Tanaka E, Maruyama K, Iwatsuru M. Enhanced Encapsulation of Amphotericin B into Liposomes by Complex Formation with Polyethylene Glycol Derivatives. Pharm Res. 1998;15(11):1737–42.
40. Singh R, Lillard JW. Nanoparticle-based targeted drug delivery. Exp Mol Pathol. 2009;86(3):215–23.
41. Saberi AH, Fang Y, Mcclements DJ. Effect of Salts on Formation and Stability of Vitamin E - Enriched Mini- emulsions Produced by Spontaneous Emulsification. J Agric Food Chem. 2014;62(46): 11246–53.
42. Márquez AL, Medrano A, Panizzolo LA, Wagner JR. Effect of calcium salts and surfactant concentration on the stability of water-in-oil (w/o) emulsions prepared with polyglycerol polyricinoleate. J Colloid Interface Sci. 2010;341(1):101–8.
43. Silvander M, Hellström A, Wärnheim T, Claesson P. Rheological properties of phospholipid-stabilized parenteral oil-in-water emulsions - Effects of electrolyte concentration and presence of heparin. Int J Pharm. 2003;252(1–2):123–32.
44. Sandström MC, Johansson E, Edwards K. Influence of preparation path on the formation of discs and threadlike micelles in DSPE-PEG2000/lipid systems. Biophys Chem. 2008;132(2–3):97–103.
45. Johnsson M, Hansson P, Edwards K. Spherical micelles and other self-assembled structures in dilute aqueous mixtures of Poly (ethylene glycol) lipid. J Phys Chem B. 2001;105:8420–30.
46. Tokudome Y, Uchida R, Yokote T, Todo H, Hada N, Kon T, et al. Effect of topically applied sphingomyelin-based liposomes on the ceramide level in a three-dimensional cultured human skin model. J Liposome Res. 2010;20(1):49–54.
47. Villasmil-Sánchez S, Rabasco AM, González-Rodríguez ML. Thermal and 31P-NMR studies to elucidate sumatriptan succinate entrapment behavior in phosphatidylcholine/cholesterol liposomes. Comparative 31P-NMR analysis on negatively and positively-charged liposomes. Colloids Surf B: Biointerfaces. 2013;105:14–23.
48. Eichner A, Stahlberg S, Sonnenberger S, Lange S, Dobner B, Ostermann A, et al. Influence of the penetration enhancer isopropyl myristate on stratum corneum lipid model membranes revealed by neutron diffraction and 2H NMR experiments. Biochim Biophys Acta Biomembr. 2017;1859(5):745–55.
49. Leal C, Rögnvaldsson S, Fossheim S, Nilssen EA, Topgaard D. Dynamic and structural aspects of PEGylated liposomes monitored by NMR. J Colloid Interface Sci. 2008;325(2):485–93.
50. Voronov VK. NMR spectra transformed by electron-nuclear coupling as indicator of structural peculiarities of magnetically active molecular systems. J Phys Chem A. 2016;120(34):6688–92.
51. Todo H, Kimura E, Yasuno H, Tokudome Y, Hashimoto F, Ikarashi Y, et al. Permeation pathway of macromolecules and nanospheres through skin. Biol Pharm Bull. 2010;33(8):1394–9.
52. Bos JD, Meinardi MMHM. The 500 Dalton rule for the skin penetration of chemical compounds and drugs. Exp Dermatol. 2000;9(3):1–5.
53. Bouwstra JA, Honeywell-Nguyen PL, Gooris GS, Ponec M. Structure of the skin barrier and its modulation by vesicular formulations. Vol. 42. Prog Lipid Res. 2003;42(1):1–36.
54. Honeywell-Nguyen PL, Bouwstra JA. Vesicles as a tool for transdermal and dermal delivery. Drug Discov Today Technol. 2005;2(1):67–74.
55. Iino H, Fujii M, Fujino M, Kohara S, Hashizaki K, Kira H, et al. Influence of Characteristics of Oily Vehicle on Skin Penetration of Ufenamate. Biol Pharm Bull. 2017;40(2):220–6.